Atmospheric Environment 48 (2012) 184–194

Contents lists available at ScienceDirect

Atmospheric Environment

journal homepage: www.elsevier.com/locate/atmosenv

The ash dispersion over Europe during the Eyjafjallajökull eruption – Comparison of CMAQ simulations to remote sensing and air-borne in-situ observations

Volker Matthias [a,*], Armin Aulinger [a], Johannes Bieser [a], Juan Cuesta [b,c], Beate Geyer [a], Bärbel Langmann [e], Ilya Serikov [f], Ina Mattis [g], Andreas Minikin [h], Lucia Mona [d], Markus Quante [a], Ulrich Schumann [h], Bernadett Weinzierl [h]

[a] Helmholtz-Zentrum Geesthacht, Institute of Coastal Research, Max-Planck-Straße 1, 21502 Geesthacht, Germany
[b] Laboratoire Inter-Universitaire des Systèmes Atmosphériques (LISA), Université Paris Est Créteil (UPEC) 61, Avenue du Général de Gaulle, 94010 Créteil Cedex, France
[c] Laboratoire Atmospheres Milieux Observations Spatiales (LATMOS), 4 Place Jussieu, 75252 Paris, France
[d] Consiglio Nazionale delle Ricerche – Istituto di Metodologie per l'Analisi Ambientale (CNR-IMAA), C. da S. Loja, I-85050 Tito Scalo, Potenza, Italy
[e] Institute of Geophysics, University of Hamburg, Klima Campus, Bundesstraße 55, 20146 Hamburg, Germany
[f] Max-Planck-Institut für Meteorologie, Bundesstraße 55, 20146 Hamburg, Germany
[g] Leibniz Institute for Tropospheric Research, Permoserstraße 15, 04318 Leipzig, Germany
[h] Deutsches Zentrum für Luft-und Raumfahrt (DLR), Institut für Physik der Atmosphäre, Münchner Straße 20, 82230 Oberpfaffenhofen, Germany

ARTICLE INFO

Article history:
Received 15 February 2011
Received in revised form
24 June 2011
Accepted 29 June 2011

Keywords:
Volcanic eruption
Ash dispersion
Chemistry transport model
Lidar
Sun photometer
Ash concentration

ABSTRACT

The dispersion of volcanic ash over Europe after the outbreak of the Eyjafjallajökull on Iceland on 14 April 2010 has been simulated with a conventional three-dimensional Eulerian chemistry transport model system, the Community Multiscale Air Quality (CMAQ) model. Four different emission scenarios representing the lower and upper bounds of the emission height and intensity were considered. The atmospheric ash concentrations turned out to be highly variable in time and space. The model results were compared to three different kinds of observations: Aeronet aerosol optical depth (AOD) measurements, Earlinet aerosol extinction profiles and in-situ observations of the ash concentration by means of optical particle counters aboard the DLR Falcon aircraft. The model was able to reproduce observed AOD values and atmospheric ash concentrations. Best agreement was achieved for lower emission heights and a fraction of 2% transportable ash in the total volcanic emissions. The complex vertical structure of the volcanic ash layers in the free troposphere could not be simulated. Compared to the observations, the model tends to show vertically more extended, homogeneous aerosol layers. This is caused by a poor vertical resolution of the model at higher altitudes and a lack of information about the vertical distribution of the volcanic emissions. Only a combination of quickly available observations of the volcanic ash cloud and atmospheric transport models can give a comprehensive picture of ash concentrations in the atmosphere.

1. Introduction

Volcanoes are the by far largest point sources on Earth that emit particles (ash) and gases, in particular sulphur dioxide into the atmosphere. Their emission strength is highly variable in time. Typically high emissions take place for only few days or weeks while they are very low most of the time. High volcanic ash concentrations in the atmosphere lead to low visibility, reduced solar radiation reaching the surface and might cause negative health effects for people who were exposed to high ash concentrations in air. Most of these effects are quite local, only very huge eruptions that emit particles and sulphur dioxide directly into the stratosphere may have long lasting effects on the solar radiation and thus on climate.

During the eruption of the Icelandic volcano Eyjafjallajökull between 14 April and 22 May 2010 the volcanic ash was transported into regions with high air traffic density. This was particularly the case in the beginning of the eruption phase when strong northwesterly winds transported high amounts of aerosol particles to Central Europe. The air space over Europe was almost completely closed between 16 April and 21 April 2010 causing high losses for the airlines. Also other industries that rely on the timely delivery of necessary components faced problems to maintain their production. Numerous air passengers were stuck at the airports and could not reach their destination. In the following the airlines claimed

* Corresponding author. Tel.: +49 4152 872346; fax: +49 4152 872332.
E-mail address: volker.matthias@hzg.de (V. Matthias).

1352-2310/$ – see front matter © 2011 Elsevier Ltd. All rights reserved.
doi:10.1016/j.atmosenv.2011.06.077

that the grounding of the aircrafts was not justified because the ash concentrations were low and would not cause any damage to the turbines of their jets. However, it was not clear how high the ash concentrations were and neither the Volcanic Ash Advisory Center (VAAC) that is responsible for the calculation of the ash dispersion by means of atmospheric models, nor any other institution could give reliable numbers of the aerosol concentration and the altitude of the aerosol layers in the free troposphere.

Three-dimensional dynamical numerical models can help to get a more comprehensive picture of the ash distribution in the atmosphere after a volcanic eruption (see e.g. Stohl et al., 2011; Emeis et al. (2011)). Chemistry transport models are capable of simulating the transport of small particles in the atmosphere provided the necessary input parameters are at hand. These are accurate three dimensional meteorological and emission fields. Meteorological fields can be simulated with mesoscale models which are driven by global reanalysis data that is available shortly after atmospheric observations have been reported. The models can also be applied in forecast mode giving the possibility to calculate the ash distribution in real time or to forecast the development of the ash cloud. The largest uncertainties are connected with the emission strength and the altitudes up to which the ash is emitted by the volcanic eruption. It is possible to estimate the emission heights by visual inspection or by radar observations in the vicinity of the volcano, the amount of the emitted ash can then be assessed by simple empirical relations between emission height and emission intensity. Only a minor part of the emitted particles are small enough that they may be transported over several thousands of kilometres in the upper troposphere. This size fraction is again subject to large uncertainties. Therefore it is highly recommendable to compare the results of the ash transport simulations to all observations that are available to assess the uncertainties connected with the emissions that feed the simulation. If this can be assured, the simulations can be used to give an estimate about the distribution of the ash concentrations in the atmosphere in space and time.

This paper describes simulations of the ash transport of the Eyjafjallajökull volcanic eruption between 14 April and 22 May 2010. The calculations have been done with a conventional Eulerian chemistry transport model, the Community Multiscale Air Quality (CMAQ) model. The model system together with its input parameters is described in section 2 of this paper. The capability of the model system to give a comprehensive picture of the ash distribution over Europe has been tested. The observational data that was compared to the model results includes sun photometer measurements, lidar profiles and in-situ observations of the ash concentrations aboard an aircraft. It is described in section 3 while the simulation results and their comparison to the observations are discussed in section 4.

2. Model description

2.1. Chemistry transport model

CMAQ has originally been developed to study air pollution episodes, in particular ozone episodes, in the United States. It has been further developed in recent years to simulate pollution by aerosol particles, heavy metals and mercury but it has not been built or adapted to treat especially volcanic ash transport in high altitudes. The model includes gas phase, aerosol and aqueous chemistry, primary and secondary particles and it is widely used to simulate atmospheric transport of particles. It should therefore in principle be suited to treat volcanic ash transport, too. In this study, the CBM4 chemical mechanism (Gery et al., 1989) is used. The aerosol is represented by 11 different classes and three size modes (Aitken, accumulation and coarse mode). Each of them is assumed to have a lognormal distribution. Volcanic ash is best represented by coarse mode aerosol particles. In CMAQ they have a geometric mean diameter of 6 μm, the standard deviation of the logarithm of the particle size is 2.2.

For our study the CMAQ model was set up on a 24×24 km^2 grid for Northwest Europe. This model domain was nested into a larger 72×72 km^2 grid covering Europe and parts of North Africa. Thirty vertical levels up to 20 hPa with 20 levels below approx. 2500 m were used in a terrain following σ-pressure co-ordinate system. In the vertical, this is the standard setup of the model as it has been used for simulations of the aerosol distribution and benzo(a)pyrene concentrations in Europe (Matthias, 2008; Matthias et al., 2009).

2.2. Emissions

The emissions of the Eyjafjallajökull volcano were estimated based on an empirical relationship between plume height and the eruption volume rate given by Mastin et al. (2009). Both emission heights and resulting tephra flux are presented in the introductory paper to this special issue (Langmann et al., 2012). The uncertainty range has been considered by performing four model runs that are defined by the upper and lower limits of the emission heights (called MIN and MAX emission cases) and the upper and lower limits of the fraction of transportable ash related to the total tephra emissions. Measured grain size distributions close to Eyjafjallajökull (http://www.earthice.hi.is/page/ies_EYJO2010_Grain) show mass contributions from about 1 to 4% for PM10 during the first eruption phase. Here, because also particles larger than 10 μm were considered, the lower limit was assumed to be 2% of the total tephra emissions (MIN2 and MAX2 emissions), the upper limit to be 4% of the total tephra emissions (MIN4 and MAX4 emissions). Time series of the emission height and emission strength are shown in Fig. 1. It has been assumed that volcanic ash is emitted into all heights between the altitude of the volcano and the estimated maximum emission height with largest emissions in the uppermost altitudes (Fig. 1c). The total emissions between 14 April and 22 May 2010 considered as coarse mode aerosol are 15 and 30 Tg for the MIN2 and MIN4 cases and 25.5 and 51 Tg for the MAX2 and MAX4 cases. These numbers are well within the range of 2–50 Tg (best estimate 10 Tg) derived by Schumann et al. (2011) based on airborne observations close to the volcano. New attempts to derive time- and height-resolved volcanic ash emissions from a combination of satellite images and atmospheric transport models have only become available very recently (Stohl et al., 2011) and could not be considered here.

Emissions from anthropogenic sources as well as biogenic emissions were also taken into account in the model simulations. Their consideration allows for a better comparison of the model results to ground based sun photometer observations. Anthropogenic emissions are based on EMEP and EPER emissions reports and have been processed using the emission model SMOKE for Europe (Bieser et al., 2010), biogenic emissions depend on land use (e.g. tree species), solar radiation and temperature. They are calculated based on Guenther et al. (1995) in the SMOKE for Europe emission model. Sea salt is parameterized in CMAQ using a wind speed dependent approach.

2.3. Initial and boundary conditions for CMAQ

CMAQ was run on a 72×72 km^2 grid for the entire European continent. The results of this model run served as boundary conditions for the inner 24×24 km^2 grid. By this it could be guaranteed that aerosol particles that are transported out of the inner domain are not lost but may be re-advected through the

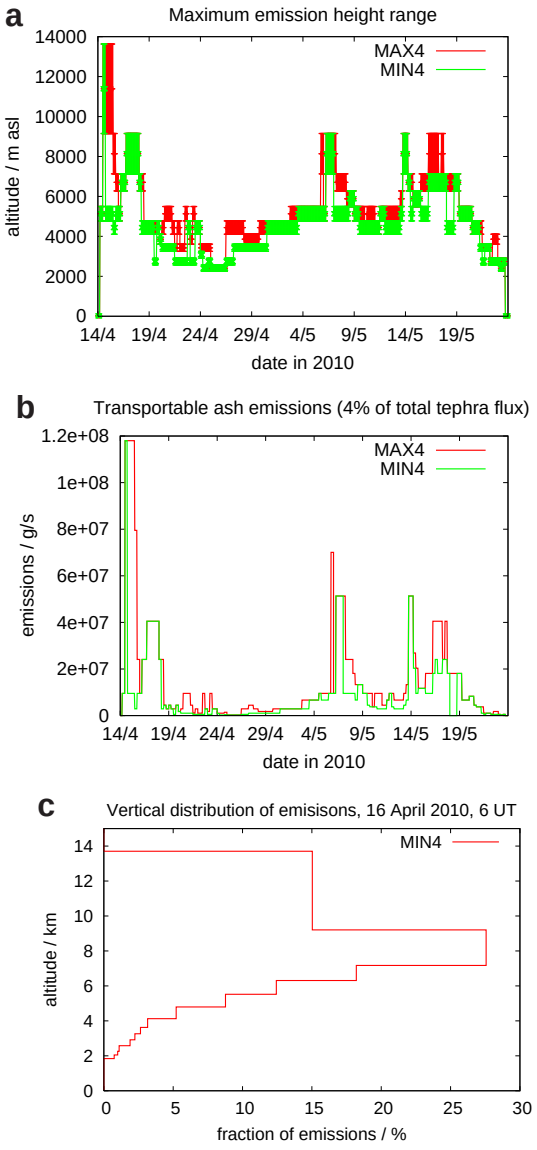

Fig. 1. Volcanic emissions as described in Langmann et al., (2012): a) maximum emission heights b) total transportable ash emissions for the MIN4 and MAX4 cases and c) vertical distribution of the MIN4 emissions on 16 April 2010, 6 UT. The coloured area in a) denotes the extension of the vertical layer. The MIN2 and MAX2 cases exhibit half of the emissions of the MIN4 and MAX4 cases, respectively, but in the same height intervals. (For interpretation of the references to colour in this figure legend, the reader is referred to the web version of this article.)

boundaries. The boundary conditions for the outer grid were constant at all borders. Climatological vertical profiles were used for CO, O_3, NO_2, NO, HNO_3, SO_2, SO_4, PAN, NH_3, and formaldehyde.

2.4. Meteorological fields

The meteorological fields were derived from a simulation with the regional non-hydrostatic atmospheric circulation model COSMO-CLM 4.8 (Rockel et al., 2008). The simulation area covers Europe including the Mediterranean Sea to the south and most part of Greenland to the northwest. The model was run with a spatial resolution of 0.22° × 0.22° and 40 vertical levels were used within a terrain following coordinate system. The height of the uppermost level is about 27 km, the lowest level is about 20 m above ground. The simulation is driven by NCEP-1 6-hourly global reanalysis data (Kalnay et al., 1996) on a 1.875° × 1.875° grid, the output interval is 1 h.

3. Measurement data

3.1. Sunphotometer

The optical properties of aerosol particles in the entire atmospheric column are routinely observed within the Aerosol Robotic Network (Aeronet) (Holben et al., 1998). The network has grown to more than 200 stations world wide since the late 1990s and supplies a good continental coverage within Europe. The instruments can only deliver data during daytime and during totally cloud free periods, because they rely on extinction measurements of the direct and scattered solar radiation. The typical uncertainty in the measured aerosol optical depth (AOD) is 0.01–0.02 (Eck et al., 1999; Holben et al., 2001). The data is submitted once a day via satellite or internet to the NASA data base in Greenbelt/Maryland, USA. It can be accessed via the Aeronet web page (http://aeronet.gsfc.nasa.gov) and is typically available the day after the observations have been made. A cloud screening of the measurements is done automatically shortly after the data submission. The result is called level 1.5 data. It can already be used for comparisons to other observations or to modelled AOD data. The final quality control is done after another calibration of the instruments which is done once a year. Afterwards the highest level 2 of the data quality is reached.

Besides the most important information about the AOD, other data products might be available, depending on cloud amount and the AOD value. During the eruption of the Eyjafjallajökull, the sky over Central Europe was cloud-free for many days. Therefore it was possible to derive a size dependent aerosol optical depth. This allowed for a detection of days when the total AOD was influenced by volcanic ash. A comparison of the modelled AOD to the Aeronet observations was done for a number of selected stations in Central and Northern Europe. An overview of these stations is given in Table 1.

3.2. Lidar

Lidar instruments are ideally suited to observe aerosol layers in higher altitudes. The quantity that is primarily observed is the aerosol backscatter coefficient at one or more wavelengths between the UV and the infrared. They can give information about the vertical extent of the aerosol layer and about its development in time. They can be operated during day and nighttime. Many instruments have the capability to determine aerosol extinction and backscatter simultaneously at nighttime using the detection of

Table 1
Location and altitude of the Aeronet stations used for a comparison of AOD.

Code	Country	Station name	Latitude North	Longitude East	Altitude/m
BEL	Poland	Belsk	51.84	20.79	190
CAB	The Netherlands	Cabauw	51.97	4.92	−1
CHI	United Kingdom	Chilbolton	51.14	−1.44	88
HAM	Germany	Hamburg	53.57	9.97	105
HEL	Germany	Helgoland	54.18	7.88	33
LEI	Germany	Leipzig	51.35	12.43	125
LIL	France	Lille	50.62	3.15	60
MIN	Belarus	Minsk	53.92	27.60	200
MUN	Germany	Munich	48.15	11.57	533
PAL	France	Palaiseau	48.70	2.21	156
WYW	United Kingdom	Wytham Woods	51.77	−1.33	160

Raman scattered light. This allows for the determination of the extinction to backscatter ratio (so called lidar ratio), which contains information about the microphysical properties of the aerosol. Assuming the lidar ratio doesn't change rapidly in time, the values observed at nighttime may be used to calculate fairly reliable extinction profiles also at daytime.

The lidar observations used in this study were derived in the framework of the European Aerosol Research Lidar Network (Earlinet) (Bösenberg et al., 2003) that was established in 2000. Regular lidar observations at 27 stations in Europe are performed within this network. The data needs careful evaluation and is therefore not quickly available but it can be used upon request. Descriptions of the equipment at the different stations can be found e.g. in Papayannis et al. (2008); Mona et al. (2009); Mattis et al. (2004). Here, lidar observations at Hamburg, Leipzig, Palaiseau and Potenza are compared to model results. Details are summarized in Table 2.

3.3. In-situ aircraft observations

Several research flights have been undertaken with the DLR Falcon aircraft during the Eyjafjallajökull eruption to observe the ash cloud and to determine its microphysical, optical and chemical properties (Schumann et al., 2011). This included lidar observations from above the ash cloud, optical observations of the size spectrum within the cloud and the collection of ash samples on filters that could be analyzed in the laboratory. The observations of the size spectrum also allowed for an estimate of the aerosol mass concentrations. This quantity is directly comparable to the model results. Depending on the refractive index of the scattering ash particles, the derived aerosol mass concentrations may be connected with some uncertainties. A detailed discussion about the error margins was done by Schumann et al. (2011). Here we compare our model concentration results to the revised mass concentrations.

4. Model results

The model has been run for the period from 2 April 2010 until 23 May 2010. The model runs included anthropogenic emissions in order to facilitate comparisons of the total optical depth to the model results. The first 12 days up to 14 April, the day of the main eruption of the Eyjafjallaökull volcano, were calculated to produce aerosol concentration fields that are almost independent from the initial conditions. For the following period from 14 April until 23 May, four runs with different assumptions about the rate and height of the volcanic emissions were performed (see section 2.2).

4.1. Ash dispersion

The initial volcanic ash emissions were transported eastwards and reached the Norwegian coast in the morning of 15 April. After a turn in wind direction to Northwest in the evening of 14 April, the volcanic ash was rapidly transported in a rather narrow corridor via the North Sea to Denmark and Northern Germany where it arrived in the evening of 15 April (Fig. 2a). It was then transported southwards and was located over South Germany, large parts of France and the Benelux countries on 16 and 17 April where it resided approximately until 19 April (Fig. 2b). Steady winds from North and Northwest over Iceland and the North Sea favoured a continued transport of ash particles towards Central Europe until 20 April. Afterwards the emissions were lower and with changing wind directions, only small amounts of ash were transported to the European continent until the beginning of May. Between 2 and 5 May the United Kingdom was largely influenced by stronger emissions in this second phase of the eruption (Fig. 2c and d). In the following, large amounts of ash particles were first transported southwards and then eastwards influencing mainly the Mediterranean region. Parts of the ash entered again Central Europe from the Southwest on 8 and 9 May. During the last stronger eruption phase between 14 and 18 May volcanic ash was like in the beginning of the eruption transported southeastwards and reached the UK the same day while the ash was located over Germany and France between 16 and 18 May (Fig. 2e and f).

The modelled ash dispersion has been compared to forecasts provided by the Volcanic Ash Advisory Center (VAAC) in London. The VAAC uses the Lagrangian NAME model to simulate the transport and the distribution of volcanic emissions (Witham et al., 2007). They use standard release rates and define the borders of the modelled ash cloud from a visual ash-cloud look-up table provided by NOAA. Hazardous ash concentration is determined as a function of the plume height, but no concentration values were given in the forecasts in April 2010. Fig. 3 exemplarily shows the ash distribution on 17 April 2010 at 18 UT. The VAAC map is a forecast of the ash distribution in three different height ranges (0–20,000 ft, 20,000–35,000 ft, and 35,000–55,000 ft) published 6 h before 18 UT while the CMAQ model result shows the integrated ash concentration between 2000 and 13,000 m asl for the emission scenario MIN2. It can be seen that both models give the same overall picture. Even a rather complex pattern of the ash distribution with some smaller ash free regions over the North Sea and some small tongues of ash reaching France and North Ireland are displayed in both model results. The VAAC forecast shows regions with ash over Central Europe which do not appear in the CMAQ simulations (Fig. 3a). One reason for this is the threshold level of 100 mg m^{-2} of integrated ash concentration below which no ash is displayed. It is not clear which threshold level was used for the VAAC forecast because ash concentrations were not available. Another reason could be a mismatch in time. The ash cloud was travelling southwards in Central Europe. In the morning of 17 April 2010 the ash concentrations were much higher in that region.

4.2. Optical depth

In order to compare the model results to observations at several locations in Europe, the modelled atmospheric aerosol concentrations in the entire troposphere have been converted into aerosol optical depth values. A rather simple approach proposed by Malm et al. (1994) is used to calculate the aerosol extinction in the mid-visible spectrum around 500 nm wavelength. The extinction coefficient depends on aerosol mass and humidity in the following way:

Table 2
Lidar data used for comparisons to model data.

Station name	Country	Latitude North	Longitude East	Time window/UT	Quantity
Hamburg	Germany	53.57	9.97	16 April 2010, 5:30–5:57	Extinction at 532 nm
Leipzig	Germany	51.35	12.43	16 April 2010, 11:56–17:30	Backscatter at 532 nm
Palaiseau	France	48.7	2.21	18 April 2010, 2:30–3:30	Backscatter at 532 nm
Potenza	Italy	40.60	15.72	20 April 2010, 22:00–22:30	Backscatter at 532 nm

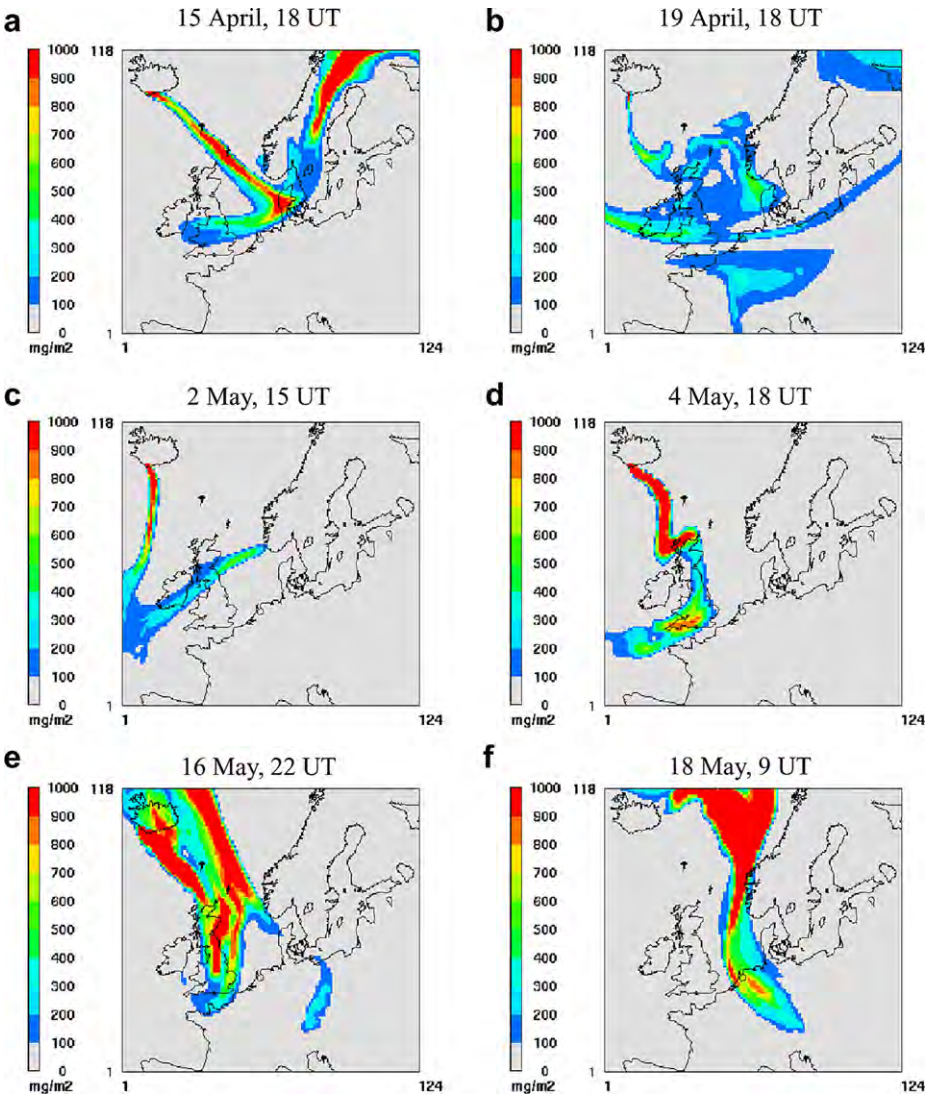

Fig. 2. Temporal development of the ash cloud over Europe between 15 April and 18 May 2010 as reproduced with the CMAQ model. Given is the total ash column above 2000 m for the MIN2 emission case.

$$\alpha_{\text{ext}} = 0.003f(\text{RH})\left(m_{\text{NH}_4} + m_{\text{NO}_3} + m_{\text{SO}_4}\right) + 0.004m_{\text{OM}} + 0.01m_{\text{EC}} + 0.001m_{\text{PM2.5}_{\text{oth}}} + 0.0006m_{\text{PM}_{\text{coarse}}} \quad (1)$$

where m_x denotes the mass m of species X which are ammonium (NH_4), nitrate (NO_3), sulphate (SO_4), organic matter (OM), elemental carbon (EC), other accumulation mode aerosols ($PM2.5_{oth}$) and all coarse mode aerosol (PM_{coarse}). The relative humidity correction $f(\text{RH})$ is described by Malm et al. (1994) and it is provided in look-up tables. It varies between 1 (at low RH) and 21 (at RH = 99%). All coefficients in Eq. (1) are given in $m^2\ mg^{-1}$. The extinction is calculated from the aerosol mass for all model layers and then vertically integrated to give the aerosol optical depth. The

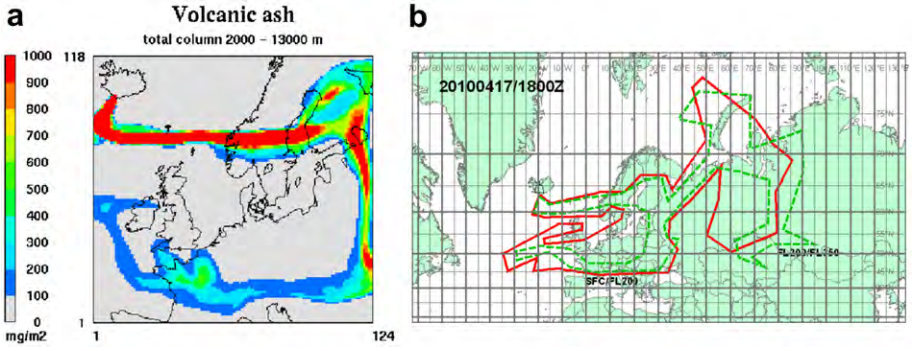

Fig. 3. Comparison of a) CMAQ model results to b) a forecast provided by the Volcanic Ash Advisory Center (VAAC) on 17 April 2010, 18 UT over Central Europe.

method has been tested by comparing modelled aerosol optical depth values to Aeronet sun photometer observations (Matthias, 2008). It turned out that the AOD is typically underestimated by about 0.1 in the planetary boundary layer (PBL) but the main reason for this is the underestimation of the aerosol mass which is in the range of about 40%. This is caused by missing organic aerosols and by too low aerosol mass in the coarse mode.

Because the volcanic ash is treated as coarse mode aerosol in the model there is no increase of the extinction by volcanic ash due to humidity growth. This is reasonable considering that the ash consists mainly of silica, aluminium oxide, iron oxide and other non-hygroscopic material and the ash plumes were often rather dry (Schumann et al., 2011). The mass to extinction ratio given by Malm et al. (1994) for coarse particles is 0.0006 m^2 mg^{-1}. Gasteiger et al. (2011) investigated this ratio for volcanic ash from the Eyjafjallajökull eruption over Munich by means of multiwavelength lidar observations. They found values ranging from 0.00043 to 0.0012 m^2 mg^{-1}, their best estimate was 0.00069 m^2 mg^{-1}.

Examples of the modelled and observed aerosol optical depth at four different stations (Hamburg, Chilbolton, Palaiseau and Leipzig) in the first phase of the eruption (14–21 April 2010) are shown in Fig. 4. All emission scenarios have been considered for the comparison. The MAX4 emissions lead to very high optical depth values of more than 2 on several days. Such high AOD values were not observed throughout the whole period. On many days the MAX2 emissions result in too high AODs, too. The AODs calculated with the MIN2 emission values are closest to the observations at most of the stations, the MIN4 emissions still result in too high modelled AODs.

A statistical evaluation for all eleven stations listed in Table 3 between 16 and 21 April reveals the lowest mean differences and the lowest root mean square (rms) error for the MIN2 emission scenario. The AOD caused by the volcanic ash cloud is in the same order of magnitude as the AOD caused by aerosol particles in the PBL. Keeping this and the fact that the AOD in the PBL is typically underestimated by the model results in mind, the MIN2 volcanic emissions might even be too high. However, the conversion from aerosol mass into extinction as described in Eq. (1) also bears some uncertainties in the mass-to-extinction coefficient. Ansmann et al. (2010) used a conversion factor of 0.00051 mg m^{-2} which would result in approx. 15% lower optical depth values for the same aerosol mass density. This would support the fact that the emitted transportable ash is somewhere between the estimates given by the MIN2 and the MIN4 scenarios.

Table 3
Comparison of modelled (four emission cases) and observed AOD at 11 selected Aeronet stations between 16 April and 21 April 2010. Given are the mean difference to the observations and the root mean square error (rmse). The data sets contain between 28 and 57 values.

Station	MIN2		MIN4		MAX2		MAX4	
	Mean diff	rmse	Mean diff	rmse	Mean diff	rmse	Mean diff	rmse
BEL	0.13	0.3	0.21	0.49	0.32	0.51	0.6	0.94
CAB	0.0	0.09	0.08	0.13	0.28	0.39	0.65	0.83
CHI	−0.09	0.16	−0.02	0.13	0.19	0.29	0.53	0.72
HAM	0.02	0.24	0.10	0.30	0.37	0.81	0.81	1.77
HEL	−0.09	0.23	0.0	0.29	0.44	1.17	1.05	2.53
LEI	0.02	0.15	0.08	0.19	0.28	0.46	0.61	0.86
LIL	−0.03	0.10	0.10	0.14	0.29	0.37	0.74	0.92
MIN	−0.14	0.48	−0.08	0.53	−0.01	0.54	0.17	0.76
MUN	−0.12	0.16	−0.03	0.11	0.21	0.33	0.62	0.82
PAL	−0.01	0.13	0.13	0.23	0.76	0.95	1.67	2.04
WYW	−0.08	0.18	−0.02	0.16	0.2	0.37	0.54	0.81

4.3. Vertical profiles

The modelled aerosol extinction profiles at visible wavelengths have been derived following Eq. (1). They have been compared to

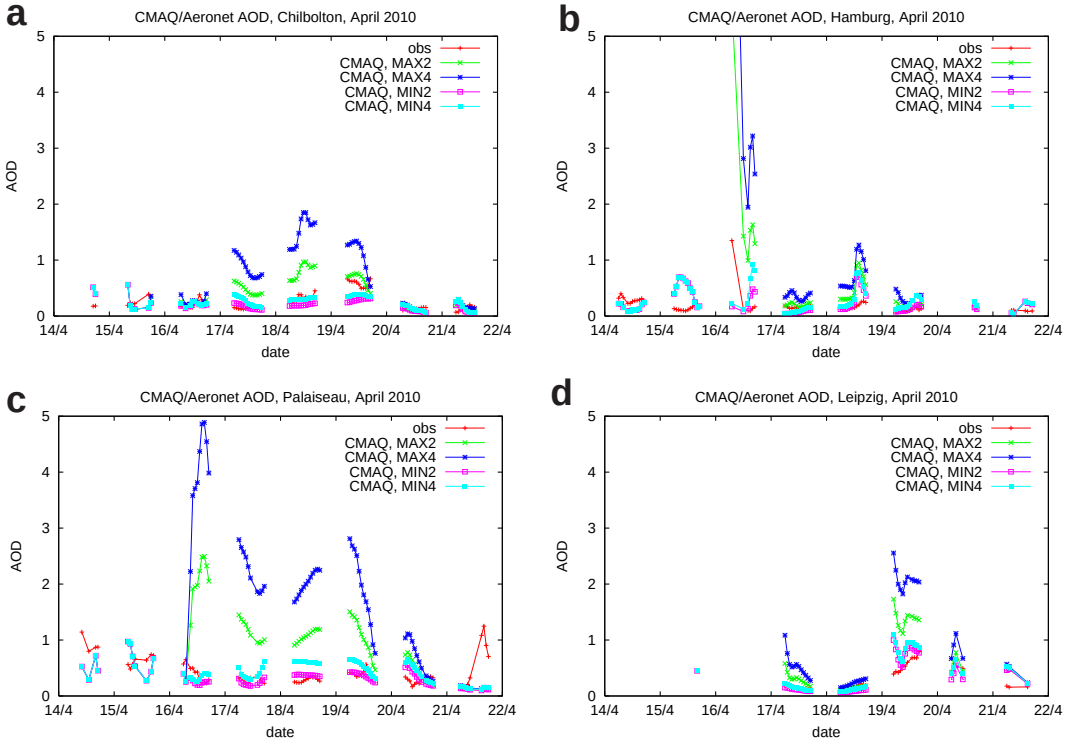

Fig. 4. Comparison of CMAQ model results to Aeronet aerosol optical depth (AOD) observations between 14 and 22 April 2010 over a) Chilbolton, b) Hamburg, c) Palaiseau, and d) Leipzig.

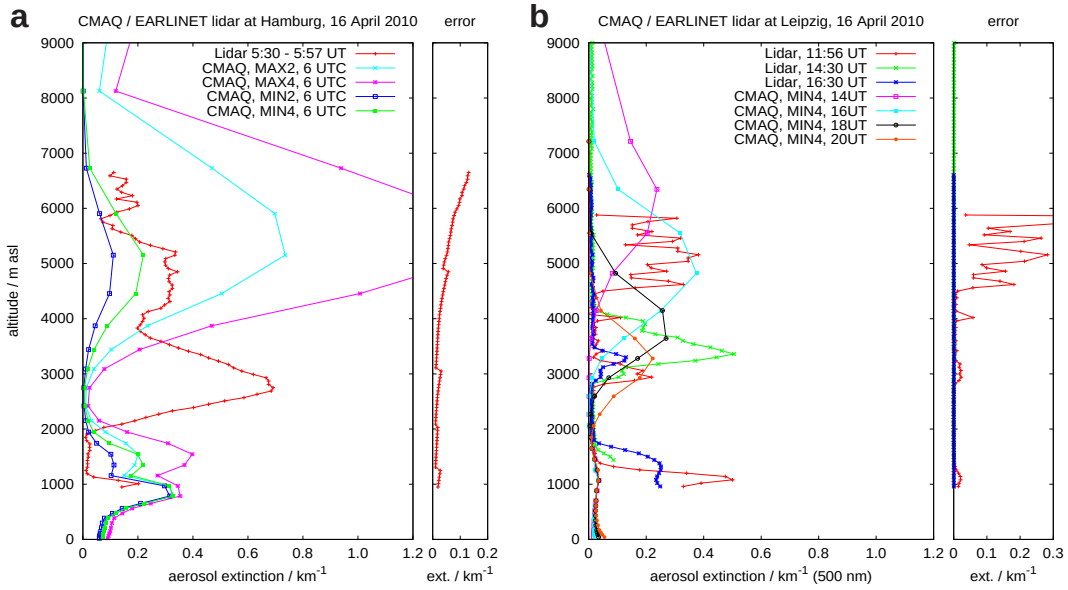

Fig. 5. Comparison of CMAQ model results to vertical aerosol profiles detected with lidar instruments at a) Hamburg on 16 April 2010, b) Leipzig on 16 April 2010.

observed aerosol extinction profiles at 532 nm which were either directly observed with the Raman Lidar technique (Ansmann et al., 1992) or deduced by multiplying the aerosol backscatter values with the lidar ratio used in the data evaluation (Fernald et al., 1972). If available, this value has been taken from Raman lidar measurements during nighttime. At Leipzig the lidar ratio was 55 sr, at Palaiseau and Potenza a value of 50 sr was taken.

The results for 16 April in Hamburg and Leipzig are shown in Fig. 5. The ash cloud reached Hamburg in the morning of 16 April, approximately 48 h after the outbreak of the volcano started. At this time the highest optical depth values of more than 1 were observed by sunphotometers at Helgoland and Hamburg (see section 4.2). The modelled profiles have been plotted for all 4 emission scenarios at 6 UT. The highest extinction peak that has been observed by the lidar in 2800 m cannot be reproduced by the model. On the other hand the modelled extinction values between 4000 and 7000 m for the scenario MIN4 match the observations quite well.

The ash cloud passed Leipzig on 16 April 2010 between 12 and 17 UT. A comparison of three lidar profiles with the modelled extinction values for the MIN4 scenario is given in Fig. 5b. The model results show an ash cloud of similar maximum extinction values around 0.3 km^{-1} that decreases in height between 14 and 20 UT. Compared to the observations, the maximum extinction values are lower and a time shift of about 4 h delay in the modelled ash cloud was found. Nevertheless the temporal development and the altitude of the ash cloud are captured quite well. Obviously, the

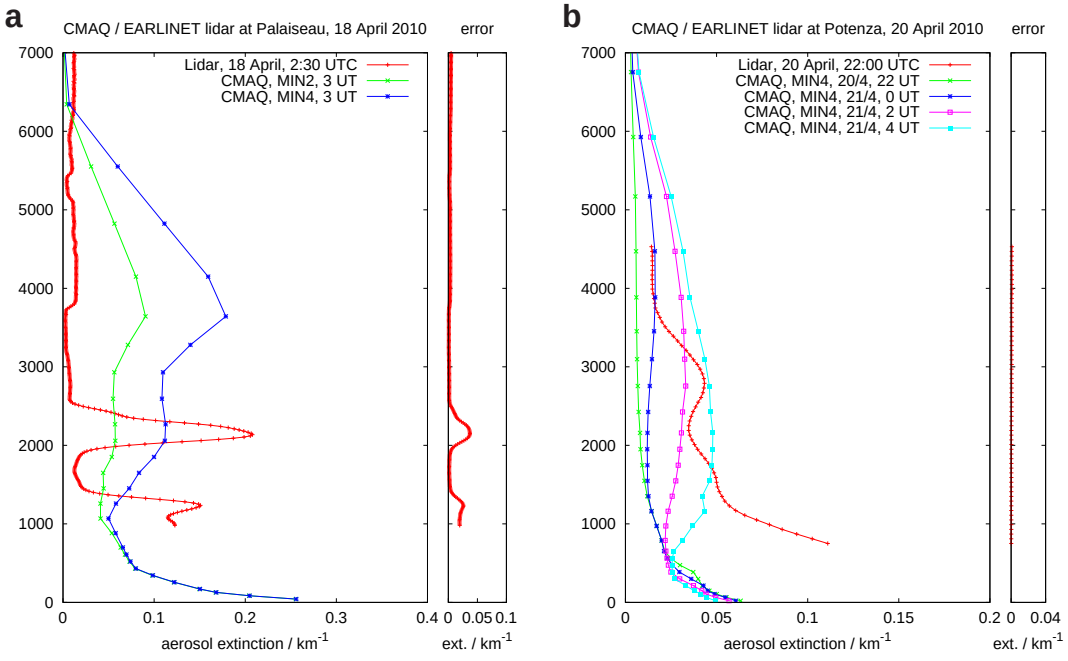

Fig. 6. Comparison of CMAQ model results to vertical aerosol profiles detected with lidar instruments at a) Palaiseau on 18 April 2010 and b) Potenza on 20 April 2010.

model is not able to represent detailed vertical structures and relatively thin aerosol layers due to a lack of vertical model resolution. This behaviour is typical for vertical extinction profiles simulated with dynamical models. It has been reported in earlier publications about comparisons of modelled aerosol vertical profiles to lidar observations (Guibert et al., 2005). Unfortunately, simultaneous sun photometer observations were not available that afternoon (see Fig. 4).

A comparison of the CMAQ model results to the lidar observations 2 days later at the SIRTA site in Palaiseau/France (Haeffelin et al., 2005) clearly demonstrates the difficulty to reproduce distinct aerosol layers (Fig. 6a). The main observed aerosol layer resides between 2000 and 2500 m asl and is about 500 m thick (see also Colette et al., 2011). Only some minor aerosol backscatter from higher altitudes was seen by the lidar. The model results, here given for the MIN2 and MIN4 emission cases, on the other hand show a broad distribution of the volcanic ash between 1000 m and 6500 m asl with slightly enhanced values between 3000 m and 5000 m. The ash cloud reached Italy on 20/21 April (Mona et al., 2011). The modelled vertical ash distribution on that day shows a similar behaviour over Potenza (Fig. 6 b). Considering a delay of 4–6 h until the ash cloud reaches the lidar station, the observed extinction values are in the same range as the model results. However, the model shows a broad vertical distribution of the ash in altitudes between 600 m and 7000 m asl while the lidar detects only low aerosol extinction values above 4000 m and higher values close to ground.

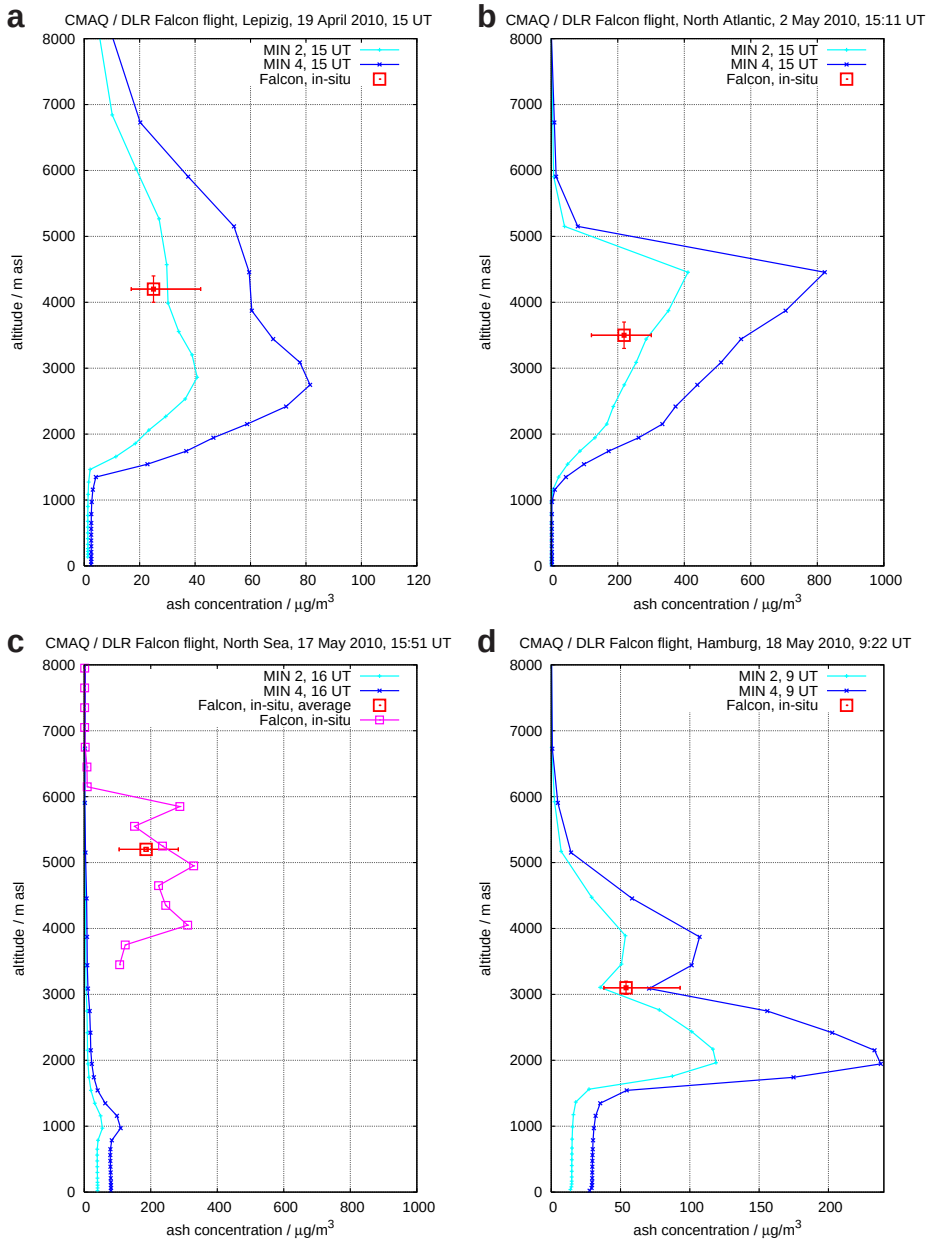

Fig. 7. Comparison of CMAQ model results to in situ observation of the ash concentration aboard the DLR Falcon over a) Leipzig on 19 April 2010, b) the North Atlantic on 2 May 2010, c) North Sea on 17 May 2010, and d) Hamburg on 18 May 2010. Red squares denote the ash concentration under the assumption of a mean value (0.004) for the imaginary part of the refractive index. Horizontal error bars for the observations show the uncertainty caused by a variation of the imaginary part of the refractive index between 0 and 0.008. Vertical bars do not indicate an error but show the vertical variation in flight altitude during the observation period. For the observations on 17 May a vertical profile of the mass concentrations is plotted. The modelled values for the emission cases MIN2 and MIN4 are given at the hour of the in situ observations. (For interpretation of the references to colour in this figure legend, the reader is referred to the web version of this article.)

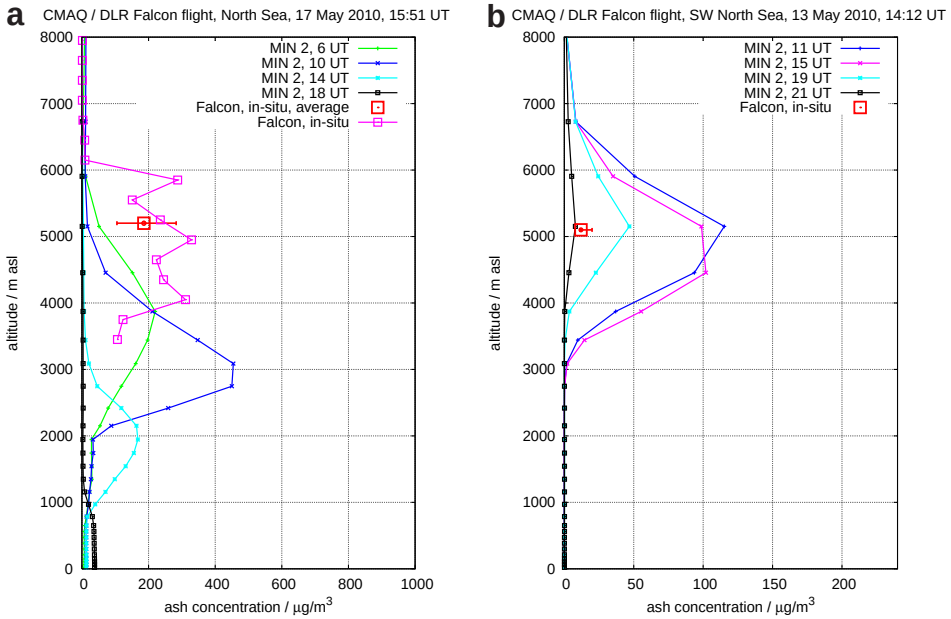

Fig. 8. Comparison of CMAQ model results to in situ observation of the ash concentration aboard the DLR Falcon over the a) North Sea on 17 May 2010 and b) SW North Sea on 13 May considering a time shift in the passage of the ash cloud. Red squares denote the ash concentration under the assumption of a mean value (0.004) for the imaginary part of the refractive index. Horizontal error bars for the observations show the uncertainty caused by a variation of the imaginary part of the refractive index between 0 and 0.008. For the observations on 17 May a vertical profile of the mass concentrations is plotted. The modelled values for the emission case MIN2 are given. (For interpretation of the references to colour in this figure legend, the reader is referred to the web version of this article.)

For the ground based lidars the statistical errors of the derived products typically increase with height because the backscattered signal gets weaker with distance. They are given in Figs. 5 and 6 together with the profiles. Aerosol extinction profiles that were derived with the Raman Lidar technique (Hamburg, 16 April, 5:30 UT and Leipzig, 16 April, 11:56 UT) show higher statistical errors because the Raman scattered signal is weaker than the aerosol backscattered signal. The error given for the lidar profile at Palaiseau was derived from Montecarlo simulations considering the main uncertainties of the retrieval like the lidar ratio and the signal calibration, too.

4.4. Ash concentrations

In-situ observations of the volcanic ash concentrations by means of optical particle counters (OPC) were performed with the DLR Falcon between 19 April and 18 May 2010. Different size ranges between 4 nm and 800 µm were covered by different instruments and measurement techniques. All details are given by Schumann et al. (2011). The mass concentrations given for 12 locations on 9 different days were compared to the model simulations. Fig. 7 exemplarily shows four simulated concentration profiles together with the observations at the time of the observations. The vertical error bars denote the given height range in which the observations were performed while the horizontal error bars give the uncertainty of the observations caused by the unknown imaginary part of the refractive index of the volcanic ash. A low absorption of the ash particles represented by a small imaginary part of the refractive index leads to the lower concentration values and vice versa for a high imaginary part. The uncertainty of the ash concentration was estimated to be a factor of two relative to the median values plotted. The model results for the MIN2 emission case match the observations in most cases very well. Typically the simulated concentrations are slightly higher than the observations.

Table 4
Comparison between modelled ash concentrations (in µg m^{-3}) for the MIN2 case and in situ observations aboard the DLR Falcon between 19 April and 18 May 2010. The range given for the observations represents different assumptions about the imaginary part of the refractive index. The range given for the model results represents the spread of model values in a time window of ±2 h around the observation time and in a vertical window of ±500 m around the observation altitude.

Location	Latitude North	Longitude East	Time window/UT	Altitude km	Observations		Model results	
					Mini	Maxi	Mini	Maxi
Leipzig	51.29	12.45	19.4., 15:08–15:15	4.2 ± 0.2	17	42	28	32
Stuttgart	48.58	9.63	19.4., 17:19–17:21	3.8 ± 0.1	13	29	35	76
Munich	47.89	11.09	19.4., 17:40–17:43	4.0 ± 0.1	12	27	29	73
Skagerrak	58.05	8.57	22.4., 19:10–19:13	2.6 ± 0.0	11	21	2	22
Baltic Sea	54.66	16.52	23.4., 12:37–12:38	2.7 ± 0.0	13	19	6	14
North Atlantic	60.17	−15.17	2.5., 15:11–15:15	3.5 ± 0.2	121	301	178	407
Munich	48.38	12.6	9.5., 14:56–15:01	4.1 ± 0.2	10	16	8	29
SW North Sea	53.41	1.45	13.5., 14:12–14:15	5.1 ± 0.0	11	20	72	114
NE England	54.76	−0.17	16.5., 14:08–14:16	6.1 ± 0.4	19	40	20	44
North Sea	52.83	2.92	17.5., 15:51–16:58	5.2 ± 1.6	105	283	1	5
Hamburg	53.17	9.12	18.5., 9:23–9:31	3.1 ± 0.1	38	93	23	82
Stuttgart	48.87	9.97	18.5., 10:13–10:17	5.2 ± 0.1	16	38	8	101

Table 5
Comparison between modelled ash concentrations (in μg m^{-3}) and in situ observations aboard the DLR Falcon considering a time shift in the model results of ±10 h and a height range of −1600 and +800 m for the observations on 17 May over the North Sea.

Location	Latitude North	Longitude East	Time window/UT	Altitude km	Observations		Model results	
					Mini	Maxi	Mini	Maxi
SW North Sea	53.41	1.45	13.5., 14:12–14:15	5.1 ± 0.0	11	20	3	115
North Sea	52.83	2.92	17.5., 15:51–16:58	5.2 ± 1.6	105	283	0.1	394

On 2 May (Fig. 7b) the aircraft flew close to the volcano in the upper part of the ash plume. The model shows much higher concentrations in upper altitudes. This is closely related to the assumptions about the emissions. On 2 May, the maximum emission height was estimated to be in 4.5–5 km asl. The vertical emission profile with highest emissions in the maximum emission height (see the example in Fig. 1c) is still visible in the concentration profile, as one would expect close to the volcano. The aircraft observations suggest that the emissions were in lower altitudes than prescribed for the model simulations.

The largest discrepancies considering all twelve cases were detected for the flight over the North Sea on 17 May. Ash concentrations between approximately 100 and 300 μg m^{-3} were observed in heights between 3.5 and 6 km while the simulations showed almost no ash in these heights at the same time (Fig. 7c). The simulations show that a horizontally rather narrow cloud with high ash concentrations passed the western North Sea in the morning of 17 May. Schumann et al. (2011) report travelling times of the ash cloud between 66 and 88 h, depending on altitude and the back-trajectory model used to derive the travel time. The CMAQ simulations 4 and 8 h before the flight show considerably higher aerosol concentrations between 200 and 500 μm m^{-3} in altitudes between 2000 m and 6000 m (Fig. 8a). However, the modelled ash cloud is in lower altitudes than it has been observed. It is not clear what the reasons for this discrepancy are but the modelled ash cloud was rather narrow and spatially inhomogeneous. As it has been seen in the comparison on 2 May the emission height is also sensitive to the vertical distribution of the ash. These uncertainties in the model results can easily lead to the observed deviations to the measurements.

Table 4 summarizes the comparisons between the modelled ash concentrations and the observations aboard the Falcon aircraft. The minimum and the maximum values of the observed concentrations as given in Schumann et al. (2011) have been compared to the range of model values for the MIN2 case in a height interval of ±500 m around the flight altitude and in a time window of ±2 h around the observation time. In most cases the range of model values in this time-height interval fits quite well with the observations. There were two exceptions, the observations over the SW North Sea on 9 May and over the North Sea on 17 May. On 13 May a mismatch in time between the model and the observations explains the large differences. If a time window of ±10 h is considered instead of ±2 h, the modelled values go down to 3 μg m^{-3} (see Table 5 and Fig. 8b). If the same time window is considered on 17 May and the height interval is taken from 3.6 to 6 km asl, the model captures also the high concentrations that were observed.

Schumann et al. (2011) also report effective diameters of the ash particles that they derived from their OPC measurements. Typical diameters of the particles were rather small, between 0.2 and 2.1 μm. Even observations in the North Atlantic area close to the volcano showed small effective diameters of 1.8 μm. These values are considerably smaller than the diameter of 6 μm that is assigned to coarse mode aerosols in CMAQ. This could lead to a quicker sedimentation of the particles in the model, on the other hand particles of 5 μm size need about two weeks to fall 1 km in the atmosphere by sedimentation (Jacobson, 1999). Thus, sedimentation should be of minor importance in ash plumes that are on average 4–5 days old (Schumann et al., 2011) and the larger particle size in the model will not affect the simulated concentrations in a significant way.

5. Conclusions

The development of the ash dispersion after the eruption of the Eyjafjallajökull volcano on Iceland on 14 April 2010 has been simulated with the three-dimensional Eulerian chemistry transport model CMAQ. Four different emission cases were considered in order to take uncertainties in the emission strength and emission height into account. The location and the extension of the ash cloud agreed well with the forecasts that were provided during the eruption phase by the Volcanic Ash Advisory Center (VAAC) in London. Comparisons of the aerosol optical depth given by the model to observations within the Aerosol Robotic Network (Aeronet) showed that the emission scenario MIN2 with lowest emissions and low emission heights gives the best agreement. This could be further verified by additional comparisons to vertical aerosol extinction profiles derived within Earlinet and in-situ observations of the ash concentrations aboard the DLR Falcon between 19 April and 18 May 2010. In some of the cases the ash cloud travelled more slowly than in reality and the model showed only good agreement to the observations if a time shift of a few hours was taken into account. It was also obvious that the model could not reproduce distinct aerosol layers of low vertical extension. The model tends to distribute the volcanic ash more or less equally over many model layers in the free troposphere. This leads to the fact that the extinction values in the MIN4 emission case agree better with the lidar values than in the MIN2 case, but the aerosol optical depth is then overestimated due to the wider vertical spread of the ash cloud. On the one hand this might be improved if more layers and therefore a better vertical resolution would be taken into account in higher altitudes. On the other hand effects of the aerosol layer on the thermal stratification, e.g. due to absorption of radiation within the aerosol layer are not taken into account in the model.

More detailed information about emission heights and the size spectrum of the emitted fine particles, that can be transported over large distances would help to simulate distinct aerosol layers more accurately. This could be achieved by lidar observations from aircraft in the vicinity of the volcano or by combining satellite imagery and atmospheric dispersion models (Stohl et al., 2011). In any case it is essential to use quickly available observations like those from Aeronet sun-photometers and combine them with model results to get reliable information about ash concentrations in the atmosphere. Neither atmospheric dispersion models nor observations alone can give a comprehensive picture of the volcanic ash distribution which is needed to manage air traffic in highly populated areas like Europe.

Acknowledgements

US EPA is gratefully acknowledged for the use of CMAQ. We thank the PIs and their staff for establishing and maintaining the 11 sites at Belsk, Cabauw, Chilbolton, Hamburg, Helgoland, Leipzig,

Lille, Minsk, Munich, Palaiseau and Wytham Woods used in this investigation.

References

Ansmann, A., Riebesell, M., Wandinger, U., Weitkamp, C., Voss, E., Lahmann, W., Michaelis, W., 1992. Combined Raman elastic-backscatter LIDAR for vertical profiling of moisture, aerosol extinction, backscatter, and LIDAR ratio. Applied Physics B 55, 18–28.

Ansmann, A., Tesche, M., Gross, S., Freudenthaler, V., Seifert, P., Hiebsch, A., Schmidt, J., Wandinger, U., Mattis, I., Muller, D., Wiegner, M., 2010. The 16 April 2010 major volcanic ash plume over central Europe: EARLINET lidar and AERONET photometer observations at Leipzig and Munich, Germany. Geophysical Research Letters 37.

Bieser, J., Aulinger, A., Matthias, V., Quante, M., Builtjes, P., 2010. SMOKE for Europe – adaptation, modification and evaluation of a comprehensive emission model for Europe. Geoscientific Model Development 3 (3), 949–1007.

Bösenberg, J., Matthias, V., Amodeo, A., Amoiridis, V., Ansmann, A., Baldasano, J.M., Balin, I., Balis, D., Böckmann, C., Boselli, A., Carlsson, G., Chaikovsky, A., Chourdakis, G., Comerón, A., Tomasi, F.D., Eixmann, R., Freudenthaler, V., Giehl, H., Grigorov, I., Hågård, A., Iarlori, M., Kirsche, A., Kolarov, G., Komguem, L., Kreipl, S., Kumpf, W., Larchevêque, G., Linné, H., Matthey, R., Mattis, I., Mekler, A., Mironova, I., Mitev, V., Mona, L., Müller, D., Music, S., Nickovic, S., Pandolfi, M., Papayannis, A., Pappalardo, G., Pelon, J., Pérez, C., Perrone, R.M., Persson, R., Resendes, D.P., Rizi, V., Rocadenbosch, F., Rodrigues, J.A., Sauvage, L., Schneidenbach, L., Schumacher, R., Shcherbakov, V., Simeonov, V., Sobolewski, P., Spinelli, N., Stachlewska, I., Stoyanov, D., Trickl, T., Tsaknakis, G., Vaughan, G., Wandinger, U., Wang, X., Wiegner, M., Zavrtanik, M., Zerefos, C., 2003. A European Aerosol Research Lidar Network to Establish an Aerosol Climatology. MPI-Report 348. Max-Planck-Institut für Meteorologie, Hamburg.

Colette, A., Favez, O., Meleux, F., Chiappini, L., Haeffelin, M., Morille, Y., Malherbe, L., Papin, A., Bessagnet, B., Menut, L., Leoz, E., Roul, L., Feb. 2011. Assessing in near real time the impact of the April 2010 Eyjafjallajökull ash plume on air quality. Atmospheric Environment 45 (5), 1217–1221.

Eck, T.F., Holben, B.N., Reid, J.S., Dubovik, O., Smirnov, A., O'Neill, N.T., Slutsker, I., Kinne, S., 1999. Wavelength dependence of the optical depth of biomass burning, urban and desert dust aerosols. Journal of Geophysical Research 104, 31333–31350.

Emeis, S., Forkel, R., Junkermann, W., Schafer, K., Flentje, H., Gilge, S., Fricke, W., Wiegner, M., Freudenthaler, V., Gross, S., Ries, L., Meinhardt, F., Birmili, W., Munkel, C., Obleitner, F., Suppan, P., 2011. Measurement and simulation of the 16/17 April 2010 Eyjafjallajökull volcanic ash layer dispersion in the northern Alpine region. Atmospheric Chemistry and Physics 11 (6), 2689–2701.

Fernald, F.G., Herman, B.M., Reagan, J.A., 1972. Determination of aerosol height distributions by lidar. Journal of Applied Meteorology 11, 482–489.

Gasteiger, J., Gross, S., Freudenthaler, V., Wiegner, M., 2011. Volcanic ash from iceland over Munich: mass concentration retrieved from ground-based remote sensing measurements. Atmospheric Chemistry and Physics 11 (5), 2209–2223.

Gery, M.W., Whitten, G.Z., Killus, J.P., Dodge, M.C., 1989. A photochemical kinetics mechanism for urban and regional scale computer modeling. Journal of Geophysical Research 94, 12925–12956.

Guenther, A., Hewitt, C.N., Erickson, D., Fall, R., Greon, C., Graedel, T., Harley, P., Klinger, L., Lerdau, M., McKay, W.A., Pierce, T., Scholes, B., Steinbrecher, R., Tallamraju, R., Taylor, J., Zimmerman, P., 1995. A global model of natural volatile organic compound emissions. Journal of Geophysical Research-Atmospheres 100 (D5), 8873–8892.

Guibert, S., Matthias, V., Schulz, M., Bösenberg, J., Eixmann, R., Mattis, I., Pappalardo, G., Perrone, M.R., Spinelli, N., Vaughan, G., 2005. The vertical distribution of aerosol over Europe – synthesis of one year of EARLINET aerosol lidar measurements and aerosol transport modeling with LMDzT-INCA. Atmospheric Environment 39 (16), 2933–2943.

Haeffelin, M., Barthes, L., Bock, O., Boitel, C., Bony, S., Bouniol, D., Chepfer, H., Chiriaco, M., Cuesta, J., Delanoe, J., Drobinski, P., Dufresne, J.L., Flamant, C., Grall, M., Hodzic, A., Hourdin, F., Lapouge, R., Lemaitre, Y., Mathieu, A., Morille, Y., Naud, C., Noel, V., O'Hirok, W., Pelon, J., Pietras, C., Protat, A., Romand, B., Scialom, G., Vautard, R., 2005. SIRTA, a ground-based atmospheric observatory for cloud and aerosol research. Annales Geophysicae 23 (2), 253–275.

Holben, B.N., Eck, T.F., Slutsker, I., Tanré, D., Buis, J.P., Setzer, A., Vermote, E., Reagan, J.A., Kaufman, Y.J., Nakajima, T., Lavenu, F., Jankowiak, I., Smirnov, A., 1998. AERONET – a federated instrument network and data archive for aerosol characterization. Remote Sensing of Environment 66, 1–16.

Holben, B.N., Tanré, D., Smirnov, A., Eck, T.F., Slutsker, I., Abuhassan, N., Newcomb, W., Schafer, J., Chatenet, B., Lavenue, F., Kaufman, Y.J., Van de Castle, J., Setzer, A., Markham, B., Clark, D., Frouin, R., Halthore, R., Karnieli, A., O'Neill, N.T., Pietras, C., Pinker, R.T., Voss, K., Zibordi, G., 2001. An emerging ground-based aerosol climatology: aerosol optical depth from AERONET. J. Geophys. Res. 106, 12067–12097.

Jacobson, M.Z., 1999. Fundamentals of Atmospheric Modelling. Cambridge University Press, Cambridge, UK.

Kalnay, E., Kanamitsu, M., Kistler, R., Collins, W., Deaven, D., Gandin, L., Iredell, M., Saha, S., White, G., Woollen, J., Zhu, Y., Chelliah, M., Ebisuzaki, W., Higgins, W., Janowiak, J., Mo, K.C., Ropelewski, C., Wang, J., Leetmaa, A., Reynolds, R., Jenne, R., Joseph, D., Mar. 1996. The NCEP/NCAR 40-year reanalysis project. Bulletin of the American Meteorological Society 77 (3), 437–471.

Langmann, B., Folch, A., Hensch, M., Matthias, V., 2012. Volcanic ash over Europe during the eruption of Eyjafjallajökull on Iceland, April-May 2010. Atmospheric Environment 48, 1–8.

Malm, W.C., Sisler, J.F., Huffman, D., Eldred, R.A., Cahill, T.A., 1994. Spatial and seasonal trends in particle concentration and optical extinction in the United States. Journal of Geophysical Research 99 (D1), 1347–1370.

Mastin, L.G., Guffanti, M., Servranckx, R., Webley, P., Barsotti, S., Dean, K., Durant, A., Ewert, J.W., Neri, A., Rose, W.I., Schneider, D., Siebert, L., Stunder, B., Swanson, G., Tupper, A., Volentik, A., Waythomas, C.F., 2009. A multidisciplinary effort to assign realistic source parameters to models of volcanic ash-cloud transport and dispersion during eruptions. Journal of Volcanology and Geothermal Research 186 (1–2), 10–21.

Matthias, V., 2008. The aerosol distribution in europe derived with the community multiscale air quality (CMAQ) model: comparison to near surface in situ and sunphotometer measurements. Atmospheric Chemistry and Physics 8, 5077–5097.

Matthias, V., Aulinger, A., Quante, M., 2009. CMAQ simulations of the benzo(a) pyrene distribution over Europe for 2000 and 2001. Atmospheric Environment 43, 4078–4086. doi:10.1016/j.atmosenv.2009.04.058.

Mattis, I., Ansmann, A., Müller, D., Wandinger, U., Althausen, D., 2004. Multiyear aerosol observations with dual-wavelength Raman lidar in the framework of EARLINET. Journal of Geophysical Research-Atmospheres 109 (D13).

Mona, L., Amodeo, A., D'Amico, G., Giunta, A., Madonna, F., Pappalardo, G., 2011. Multi-wavelength Raman lidar observations of the Eyjafjallajökull volcanic cloud over Potenza, Southern Italy. Atmospheric Chemistry and Physics Discussions 11 (4), 12763–12803.

Mona, L., Pappalardo, G., Amodeo, A., D'Amico, G., Madonna, F., Boselli, A., Giunta, A., Russo, F., Cuomo, V., 2009. One year of CNR-IMAA multi-wavelength Raman lidar measurements in coincidence with CALIPSO overpasses: level 1 products comparison. Atmospheric Chemistry and Physics 9 (18), 7213–7228.

Papayannis, A., Amiridis, V., Mona, L., Tsaknakis, G., Balis, D., Bosenberg, J., Chaikovski, A., De Tomasi, F., Grigorov, I., Mattis, I., Mitev, V., Muller, D., Nickovic, S., Perez, C., Pietruczuk, A., Pisani, G., Ravetta, F., Rizi, V., Sicard, M., Trickl, T., Wiegner, M., Gerding, M., Mamouri, R.E., D'Amico, G., Pappalardo, G., 2008. Systematic lidar observations of Saharan dust over Europe in the frame of earlinet (2000–2002). Journal of Geophysical Research-atmospheres 113 (D10).

Rockel, B., Will, A., Hense, A., 2008. The regional climate model COSMO-CLM(CCLM). Meteorologische Zeitschrift 17 (4), 347–348.

Schumann, U., Weinzierl, B., Reitebuch, O., Schlager, H., Minikin, A., Forster, C., Baumann, R., Sailer, T., Graf, K., Mannstein, H., Voigt, C., Rahm, S., Simmet, R., Scheibe, M., Lichtenstern, M., Stock, P., Rüba, H., Schäuble, D., Tafferner, A., Rautenhaus, M., Gerz, T., Ziereis, H., Krautstrunk, M., Mallaun, C., Gayet, J.-F., Lieke, K., Kandler, K., Ebert, M., Weinbruch, S., Stohl, A., Gasteiger, J., Olafsson, H., Sturm, K., 2011. Airborne observations of the Eyjafjalla volcano ash cloud over Europe during air space closure in April and May 2010. Atmospheric Chemistry and Physics 11, 2245–2279.

Stohl, A., Prata, A.J., Eckhardt, S., Clarisse, L., Durant, A., Henne, S., Kristiansen, N.I., Minikin, A., Schumann, U., Seibert, P., Stebel, K., Thomas, H.E., Thorsteinsson, T., Torseth, K., Weinzierl, B., 2011. Determination of time- and height-resolved volcanic ash emissions and their use for quantitative ash dispersion modeling: the 2010 Eyjafjallajökull eruption. Atmospheric Chemistry and Physics 11 (9), 4333–4351.

Witham, C.S., Hort, M.C., Potts, R., Servranchx, R., Husson, P., Bonnardot, F., 2007. Comparison of VAAC atmospheric dispersion models using the 1 November 2004 Grimsvötn eruption. Journal of Applied Meteorology 14, 27–38.